A ZERO-THICKNESS MORTAR/ INTERFACE FORMULATION WITH APPLICATION TO FRACTURE MECHANICS

M. de Francisco, I. Carol

Div. of Geotechnical Engineering and Geo-Sciences
School of Civil Engineering (ETSECCPB)
Technical University of Catalonia (UPC)
08034 Barcelona
ignacio.carol@upc.edu

Key words: Zero-thickness Interface, Mortar Methods, Fracture Mechanics.

Abstract. A zero-thickness mortar/interface element formulation is briefly described and demonstrated. This element may be considered as an extension of traditional zero-thickness interface element, in order to represent material interfaces located in between subdomains with non-matching FE meshes. In the context of small strain analysis, these elements may be equipped with the same type of constitutive laws as traditional interface elements. Therefore, if friction or fracture-mechanics-based laws are adopted, mortar/interface elements may be used to represent frictional sliding or cracking following the lines (surfaces) along which they have been pre-inserted. Two basic verification examples of this type are presented, showing that the model can correctly represent uniform states of stress and deformation when connecting unmatched mesh subdomains.

1 INTRODUCTION

Since they were first proposed in the late 60s in a geo-mechanical context [1], zero-thickness interface elements have been a very useful tool to represent contacts and discontinuities in a variety of engineering fields, including concrete and other quasi-brittle materials, bone tissue, etc. However, as originally proposed, interface elements are subject to the limitation that nodes on each side must be paired and perfectly matched one-to one. That is, meshes of the continuum on both sides of the interface line have to be perfectly matching and conformal meshes. This may be not a non-trivial requirement in some cases, such as for instance in the case of complex problems containing different subdomains that may be more conveniently meshed independently, or in case of meshes initially matched that may become unmatched due to large opening/sliding of the discontinuities.

One way to deal with unmatched meshes on both sides of the discontinuities, consists of the so called “mortar” elements. The concept was originally introduced by Bernardi et al in 1987 in the context of spectral discretization of domain decomposition methods [2], and was later introduced in the FEM for large-deformation contact-friction analysis and shown to preserve the optimal convergence ratio and fulfil the Babuska-Brezzi condition [3]. Initially, mortar elements were formulated on the basis of Lagrange multipliers, although later formulations are also based on penalty approach [4]. The mortar formulation described here uses a penalty approach, which makes it similar to traditional zero-thickness interface elements and in fact,

the mortar formulation developed may be considered as an extension of those elements to the case of unmatched meshes. Another advantage of the penalty approach is the possibility of using the same constitutive models as used for interface elements, and in particular, the model of normal/shear cracking model developed in [5].

2 STANDARD INTERFACE FORMULATION

The departing point for the formulation of the mortar element is the classical displacement-based zero-thickness interface element [6]. This is why this section includes a summary/reminder of that formulation, although it is recast in a way that is more convenient for the later extension to the mortar case. Figure 1 shows a linear interface element composed of two faces with two nodes per face. Although in the figure the faces are represented at a distance from each other, locations the two faces are generally coincident. A mid-plane line is defined at mid distance between the two faces, or if they coincide, at the same location. For interpolation and integration purposes, a local coordinate ξ varying from -1 to 1, is defined along the mid-plane in such a way that nodes 1 and 3 are located just across the discontinuity at the point $\xi = -1$, which is also denoted as mid-point α, and the same for nodes 2 and 4 at $\xi = 1$, which also denoted as mid-point β.

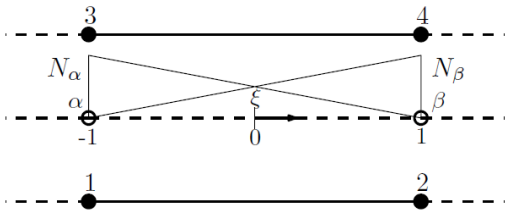

Figure 1: Geometry of standard interface element

Interface nodal relative displacement are then defined as:

$$\begin{aligned} \mathbb{r}_{\alpha}^{xy} &= \boldsymbol{u}_3 - \boldsymbol{u}_1 \\ \mathbb{r}_{\beta}^{xy} &= \boldsymbol{u}_4 - \boldsymbol{u}_2 \end{aligned} \tag{1}$$

where $\boldsymbol{u}_1$, $\boldsymbol{u}_2$, $\boldsymbol{u}_3$, $\boldsymbol{u}_4$ are the standard nodal displacements in Cartesian axes. Expression (1) may be written in matrix form as:

$$\mathbb{r}_{e}^{xy} = \begin{bmatrix} \mathbb{r}_{\alpha}^{xy} \\ \mathbb{r}_{\beta}^{xy} \end{bmatrix} = \left[\begin{array}{cc|cc} -\mathbb{I} & \mathbf{0} & \mathbb{I} & \mathbf{0} \\ \mathbf{0} & -\mathbb{I} & \mathbf{0} & \mathbb{I} \end{array}\right] \begin{bmatrix} \boldsymbol{u}_1 \\ \boldsymbol{u}_2 \\ \boldsymbol{u}_3 \\ \boldsymbol{u}_4 \end{bmatrix} = \begin{bmatrix} \mathbf{T}_A & \mathbf{T}_B \end{bmatrix} \begin{bmatrix} \boldsymbol{u}_A \\ \boldsymbol{u}_B \end{bmatrix} = \mathbf{T}\, \boldsymbol{u}_e \tag{2}$$

where $\mathbf{T}$ and $\boldsymbol{u}_e$ are the overall transfer matrix and nodal displacement vectors, while $\boldsymbol{u}_A$ and $\boldsymbol{u}_B$ are the displacement vectors containing the displacement of nodes on the upper and lower sides of the discontinuity surface, and matrices $\mathbf{T}_A$ and $\mathbf{T}_B$ are the respective transfer matrices. Relative displacements at any point ξ of the mid-plane surface are then interpolated from their mid-point nodal values using the standard shape functions $N_\alpha(\xi)$ and $N_\beta(\xi)$ (Fig.1), as:

$$\mathbb{r}^{xy}(\xi) = \begin{bmatrix} r_x(\xi) \\ r_y(\xi) \end{bmatrix} = \begin{bmatrix} N_\alpha(\xi) & 0 \\ 0 & \mathrm{N}_\alpha(\xi) \end{bmatrix} \begin{bmatrix} r_{\alpha x}(\xi) \\ r_{\alpha y}(\xi) \end{bmatrix} + \begin{bmatrix} N_\beta(\xi) & 0 \\ 0 & N_\beta(\xi) \end{bmatrix} \begin{bmatrix} r_{\beta x}(\xi) \\ r_{\alpha y}(\xi) \end{bmatrix} =$$
$$= \mathbf{N}_\alpha(\xi)\, \mathbb{r}_\alpha^{xy} + \mathbf{N}_\beta(\xi)\, \mathbb{r}_\beta^{xy} = \begin{bmatrix} \mathbf{N}_\alpha(\xi) & \mathbf{N}_\beta(\xi) \end{bmatrix} \begin{bmatrix} \mathbb{r}_\alpha^{xy} \\ \mathbb{r}_\beta^{xy} \end{bmatrix} \tag{3}$$

Combining equations (2) and (3) we obtain:

$$\mathbb{r}^{xy}(\xi) = \begin{bmatrix} \mathbf{N}_\alpha(\xi) & \mathbf{N}_\beta(\xi) \end{bmatrix} \mathbf{T}\, \boldsymbol{u}_e = \mathbf{N}(\xi)\, \boldsymbol{u}_e = [\mathbf{N}_A(\xi) \;\; \mathbf{N}_B(\xi)] \begin{bmatrix} \boldsymbol{u}_A \\ \boldsymbol{u}_B \end{bmatrix} \tag{4}$$

where $\mathbf{N}(\xi)$ is the overall interpolation matrix for the interface element, which can be decomposed in the "upper" and "lower" interpolation matrices $\mathbf{N}_A(\xi)$, $\mathbf{N}_B(\xi)$, with components:

$$\mathbf{N}_A(\xi) = \left[\begin{array}{cc|cc} -N_\alpha(\xi) & 0 & -N_\beta(\xi) & 0 \\ 0 & -N_\alpha(\xi) & 0 & -N_\beta(\xi) \end{array}\right]$$
$$\mathbf{N}_B(\xi) = \left[\begin{array}{cc|cc} N_\alpha(\xi) & 0 & N_\beta(\xi) & 0 \\ 0 & N_\alpha(\xi) & 0 & N_\beta(\xi) \end{array}\right] \tag{5}$$

The relative displacement vector in global coordinates *x,y* is rotated to the local normal and tangential coordinates *n,t* , by means of a local rotation matrix **R**:

$$\mathbb{r}^{nt}(\xi) = \mathbf{R}\, \mathbb{r}^{xy}(\xi) = \mathbf{R}\, \mathbf{N}(\xi)\, \boldsymbol{u}_e = \mathbf{B}(\xi)\, \boldsymbol{u}_e = [\mathbf{B}_A(\xi) \;\; \mathbf{B}_B(\xi)] \begin{bmatrix} \boldsymbol{u}_A \\ \boldsymbol{u}_B \end{bmatrix} \tag{6}$$

where matrix $\mathbf{B}(\xi)$ may also be decomposed into upper and lower side submatrices:

$$\mathbf{B}_A(\xi) = \mathbf{R}\, \mathbf{N}_A(\xi) \quad , \quad \mathbf{B}_B(\xi) = \mathbf{R}\, \mathbf{N}_B(\xi) \tag{7}$$

In order to obtain the element stiffness matrix, the classical procedure is followed. First, the Principle of Virtual Work (PVW) is applied along the element mid-plane surface:

$$(\delta \boldsymbol{u}_e)^T \boldsymbol{F}_e = \int_L (\delta \mathbb{r}^{nt})^T\, \mathbf{t}^{nt}\, dL \tag{8}$$

Replacing the relative displacement vector $\mathbb{r}^{nt}$ with expression (6), grouping terms around $(\delta \boldsymbol{u}_e)^T$ and eliminating this term from the equation, the weak form of equilibrium for the interface element is obtained as:

$$\boldsymbol{F}_e = \int_L \mathbf{B}^T\, \mathbf{t}^{nt} dL \tag{9}$$

The general format of a linear constitutive relation with stiffness $\mathbf{D}$ and initial stress $\mathbf{t}_0^{nt}$ is now considered as:

$$\mathbf{t}^{nt} = \mathbf{D}\, \mathbb{r}^{nt} + \mathbf{t}_0^{nt} \tag{10}$$

Replacing (9) into (8) leads to the expressions of the element stiffness matrix $\mathbf{K}_e$ and the initial force vector $\boldsymbol{F}_e^0$:

$$\boldsymbol{F}_e = \mathbf{K}_e\, \boldsymbol{u}_e + \boldsymbol{F}_e^0 \tag{11}$$

$$\mathbf{K}_e = \int_L \mathbf{B}^T\, \mathbf{D}\, \mathbf{B}\, dL \qquad , \qquad \boldsymbol{F}_e^0 = \int_L \mathbf{B}^T\, \mathbf{t}_0^{nt} dL \tag{12}$$

that may be also rephrased in terms of upper and lower B matrices:

$$\mathbf{K}_e = \int_L \begin{bmatrix}\mathbf{B}_A^T \\ \mathbf{B}_B^T\end{bmatrix} \mathbf{D}\, [\mathbf{B}_A \;\; \mathbf{B}_B] dL \qquad , \qquad \boldsymbol{F}_e^0 = \int_L \begin{bmatrix}\mathbf{B}_A^T \\ \mathbf{B}_B^T\end{bmatrix} \mathbf{t}_0^{nt} dL \tag{13}$$

3 ZERO-THICKNESS MORTAR INTERFACE

3.1 Discretization/Formulation

Zero-thickness mortar/interface elements are defined as the contact in between two continuum body surfaces denoted as "Surface A" and "Surface B", which in the general situation (and as the main difference with standard interface elements) will exhibit "unmatched" meshes (nodes on both sides will not coincide one-to-one). The contact surface itself is considered a separate entity and is called "Surface C". The discretization into mortar/interface elements is achieved by projecting all nodes from each side, surfaces A and B, onto the mid-plane surface C, and then defining one mortar element for each one of the resulting segments (Fig. 2).

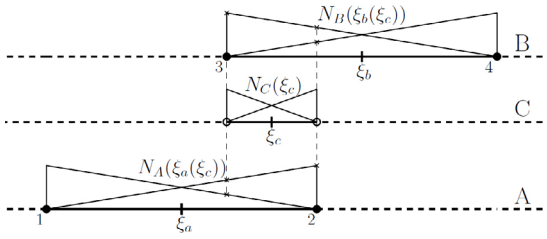

Figure 2. Geometry of mortar interface element

A standard displacement-based interpolation is defined independently for each the two sides of the mortar-interface element, with local coordinates ξ_A and shape functions $N_A^{(i)}(\xi_A)$ for surface A, and local coordinates ξ_B and shape functions $N_B^{(i)}(\xi_B)$. Additionally, a third local coordinate ξ_C also varying in the range [-1,1] is defined along the mid-plane surface of the interface/mortar element segment, as well as the corresponding interpolation functions $N_C^{(i)}(\xi_C)$. This choice of the mortar surface along the mid-plane surface has the advantage of a symmetric treatment of the two sides of the discontinuity [7,8].

Similarly to the classical interface elements, by assuming general linear constitutive behavior (10), the stiffness matrix and initial force vector of the mortar/interface element may be obtained by direct application of the PVW along the mortar surface. This leads to an expression analogous to (11), in which the stiffness and initial force vector of the mortar/interface element $\mathbf{K}_e$ and $\boldsymbol{F}_e^0$ take the form:

$$\mathbf{K}_e = \int_{L_C} \begin{bmatrix} \mathbf{B}_A^T(\xi_A) \\ \mathbf{B}_B^T(\xi_B) \end{bmatrix} \mathbf{D}[\mathbf{B}_A(\xi_A)\ \ \mathbf{B}_B(\xi_B)]\ dL_C \quad , \quad \boldsymbol{F}_e^0 = \int_{L_C} \begin{bmatrix} \mathbf{B}_A^T(\xi_A) \\ \mathbf{B}_B^T(\xi_B) \end{bmatrix} \mathbf{t}_0^{nt}(\xi_C)\ dL_C \tag{14}$$

Although formally similar to (13), the matrices in expressions (14) exhibit a fundamental difference w.r.t. those: the shape functions involved in their components are now $N_A^{(i)}$ for $\mathbf{B}_A$, which is parametrized in terms of ξ_A, and $N_B^{(i)}$ for $\mathbf{B}_B$, which is parametrized in terms of ξ_B. In spite of that, the integrals in (14) are performed over the domain of the mortar surface C, along which the position of integration points (where and constitutive stiffness, history variables, etc. are evaluated) is parametrized in terms of ξ_C. Therefore, a mapping needs to be established between ξ_C and ξ_A, and also between ξ_C and ξ_B. More details of this derivation may be found in [9].

3.2 Extension to non-linear constitutive behavior

The extension of previous elastic formulation to non-linear constitutive behavior of the mortar/interface contact surface may be achieved by means of an iterative process in which, at each iteration, $\mathbf{K}_e$ and $\boldsymbol{F}_e^0$ are recalculated to represent the new tangential stiffness and residual force vector, respectively. In this study, an existing and extensively verified normal/shear cracking constitutive model is chosen to characterize the behavior of the interface. This model is defined in terms of the normal and shear stresses, with a hyperbolic surface characterized by three geometric parameters: friction angle, cohesion and tensile strength. The evolution of these geometric parameters is controlled by a single history variable: the work spent on fracture processes. The model covers the full range of cracking from uniaxial tension to shear-compression, including those two limit situations, i.e.: (1) cracking under pure tension with zero shear stresses (Mode I) when the surface is reached along the horizontal axis; and (2) cracking under shear and very high compression when the surface is reached in its asymptotic region, where the hyperbola approaches a Coulomb criterion (Mode IIa), as depicted in Figure 3. More details of the constitutive model are given in [5,10]

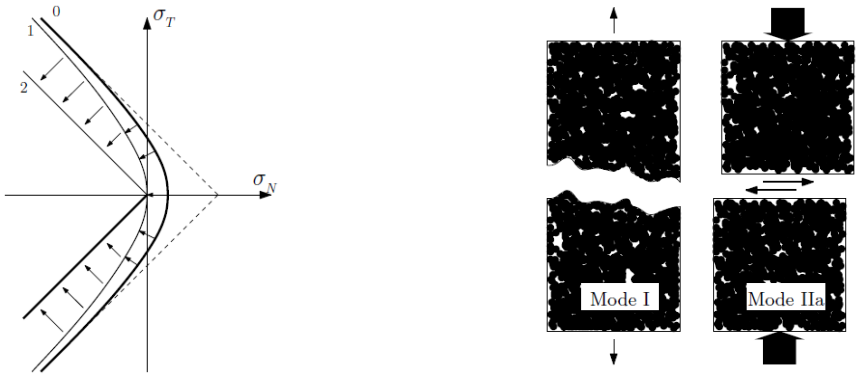

a) Evolution of cracking surface **b)** Elemental modes of fracture

Figure 3. Hyperbolic cracking model

4 NUMERICAL EXAMPLES

Two simple examples are presented in this section to illustrate that the proposed mortar interface formulation model is capable of reproducing uniform basic stress fields in spite of unmatched meshes on both sides.

4.1 Example 1: uniaxial compression test

The geometry and boundary conditions of the first example are shown in Figure 4. It consists of two horizontal layers of the same material but unmatched meshes, connected with a line of mortar/interface elements. A uniform normal stress is applied on the top face of the mesh while the bottom face remains fixed vertically, and free to expand horizontally. The parameter values used for the continuum elements are: E =10,000 MPa and $\upsilon = 0$. The only relevant interface parameters in this case are normal and tangential elastic stiffness $K_N = K_T = 1e^7$ MPa/m.

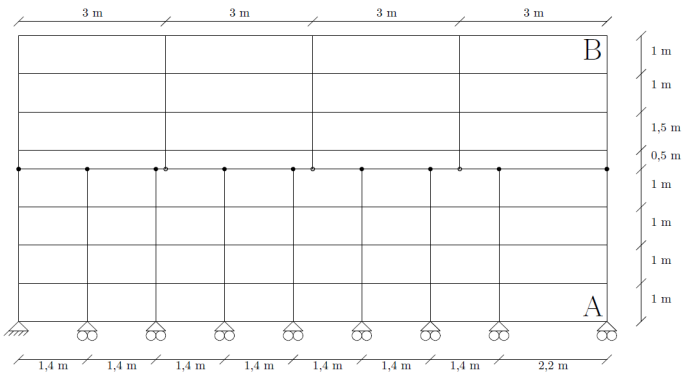

Figure 4. Example 1: geometry and boundary conditions

The results are represented in Figures 5 and 6. Fig.5 depicts the stress distribution obtained along the discontinuity line, and Figure 6 depicts the principal stresses in the continuum elements. As shown, the normal stress turns out constant and with the correct value along all mortar/interface elements and perfectly constant and well aligned in the continuum in spite of the unmatched mesh geometry.

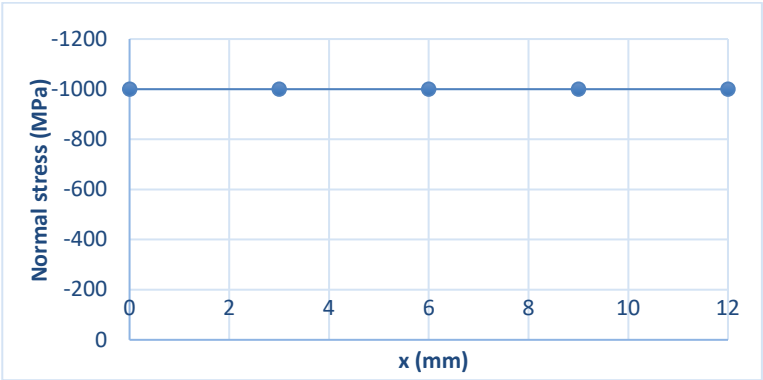

Figure 5. Compression test: normal stress along discontinuity

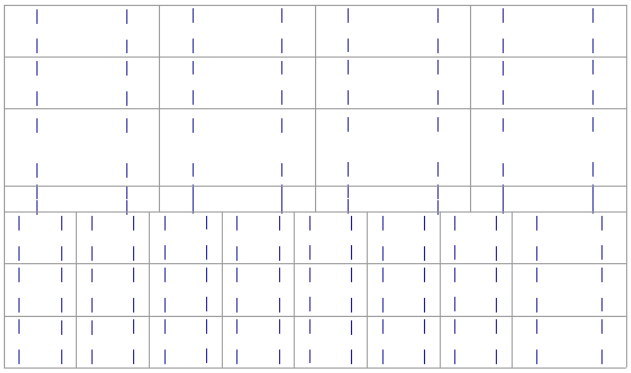

Figure 6. Compression test: principal stresses in the continuum elements.

4.2 Direct shear under high compression

The second example consists of a direct shear test, which is performed on the same geometry and as a continuation of the calculation presented in the previous example, by adding a second load step. This load consists of an increasing tangential displacement up to $\delta_t = 1.0e^{-3}$ m. applied on the nodes on the upper side of the mortar/interface line, while at the same time restricting the horizontal movement of the lower nodes of the same elements. The parameters used for the continuum and for elastic part of the interface are the same as in previous example, and the remaining parameters of the interface (now indeed relevant) are: initial friction angle $\tan\varphi_0 = 0.8785$, initial tensile strength $\chi_0 = 3.0$ MPa, initial cohesion $C_0 = 4.0$ MPa, fracture energy mode I, $G^f_I = 0.2$ MPa·m, energy mode IIa, $G^f_{IIa} = 2$ MPa·m and normal stress at which dilatancy vanishes, $\sigma_{dil} = 0$ MPa.

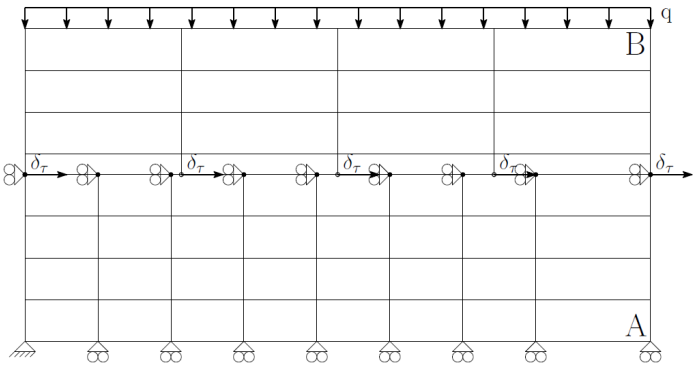

Figure 7. Direct shear under high compression: Geometry and boundary conditions

Figure 8 shows the evolution of the tangential stresses obtained at a point of the mortar/interface contact, as a function of the tangential displacement prescribed. The curve obtained directly reproduces the constitutive prediction. It has to be noted that the results show at all times uniform state of stress and deformation in both the continuum and the mortar/interface contact. Note that the results obtained are not at all trivial since, although tangential displacements may be applied to the mortar nodes directly, the normal stress is

applied on the top surface of the domain, which makes the results totally dependent on the overall correct structural response.

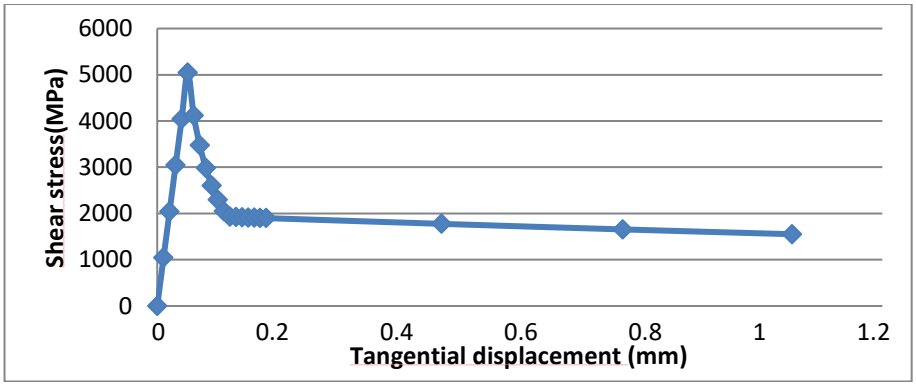

Figure 8. Results of the shear test: shear stress vs. tangential relative displacement.

5 CONCLUDING REMARKS

A general zero-thickness mortar/interface formulation is described in this paper. These elements may be used to connect continuum elements in the general case of non-conforming discretization between the elements of two sides of interface. Simple numerical examples are proposed to test the performance of the approach, and the results obtained turn out correct, that is the mortar/interface element developed succeeds in transmitting properly the compression and shear stresses applied through the interface, even in the scenario of totally unmatched meshes. The results presented are a part of a wider scope research aimed at modeling the transition between fracture of quasi-brittle materials and contact friction between the resulting fragments.

ACKNOWLEDGEMENTS

The work was partially supported by research grants BIA2016-76543-R from MEC (Madrid), which includes FEDER funds, and 2017SGR-1153 from Generalitat de Catalunya (Barcelona). The FPU fellowship from MEC (Madrid) to the first author is also greatfully acknowledged.

REFERENCES

[1] Goodman R.E., Taylor R.L., Brekke T. A model for the mechanics of jointed rock. J Soil Mech. Found. Div. Proc. ASCE (1968) 94.

[2] Bernardi C., Maday Y., Patera A.T. A new nonconforming approach to domain decomposition: the mortar element method. In H.Brezis and J. L. Lios, editors, Nonlinear Partial Differential Equations and Their Applications, Collège de France Seminar, Piman, (1987).

[3] Wohlmuth B.I. Discretization methods and iterative solvers based on domain decomposition. Springer, (2001).

[4] Yang B., Laursen T.A., Meng X.N., Two dimensional mortar contact methods for large deformation frictional sliding, Int. J. Numer. Methods Engrg. (2005) 62 1183–1225.

[5] Carol I., Prat P.C., López C.M. A normal/shear cracking model. Application to discrete crack analysis, ASCE J. Engrg. Mech. 123 (8) (1997) 765–773.
[6] Gens A., Carol I., and Alonso, E. An interface element formulation for the analysis of soil-reinforcement interaction. Computers and Geotechnics. (1988) 7:133-151.
[7] Simo J.C., Wriggers P., Taylor R.L. A perturbed lagrangian formulation for the finite element solution of contact problems. Computer Methods in Applied Mechanics and Engineering; (1985) 50:163–180.
[8] El-Abbasi N. and Bathe K. J. Stability and patch test performance of contact discretizations and a new solution algorithm. Computers and Structures, (2001) 79: 1473-1486.
[9] de Francisco, M., and Carol, I. Displacement-based and hybrid formulations of zero-thickness mortar/interface elements, with application to fracture mechanics. Manuscript in preparation.
[10] Caballero A., Willam K.J., Carol I. Consistent tangent formulation for 3D interface modeling of cracking/fracture in quasi-brittle materials. Comput. Methods Appl. Mech. Engrg. 197 (2008) 2804–2822.